



## 2011 International Conference on Physics Science and Technology (ICPST 2011) Microtube's Tapers Affect its Subwavelength Focusing Effect

Yurong Chen, Shuo Sun, Wei Fang and Jian Fu\*

*State Key Laboratory of Modern Optical Instrumentation, Department of Optical Engineering,  
Zhejiang University, Hangzhou 310027, China*

---

### Abstract

A tapered microtube fabricated from a glass capillary tube can achieve subwavelength focusing at optical frequencies. This focusing effect is influenced by many factors. The role of taper ratios is investigated in this paper with theoretical analysis and numerical simulation. It revealed that when the taper ratio is larger, the focusing spot has higher intensity and smaller FWHM.

© 2011 Published by Elsevier B.V. Open access under [CC BY-NC-ND license](http://creativecommons.org/licenses/by-nc-nd/3.0/).  
Selection and/or peer-review under responsibility of Garry Lee.

*Keywords:* subwavelength focusing; microtube; micro-nano photonics

---

### 1. Instruction

Focusing light beams with subwavelength resolution is essential to a wide range of applications such as semiconductor lithography, optical trapping [1] and high density optical data storage [2]. However, this is beyond the ability of conventional optics approach due to the so-called diffraction limit.

In the year of 2000, J. B. Pendry first introduced the concept of “superlens” [3], which makes use of ideal negative index materials (NIM) to recover the evanescent components of the light source and thus to break the fundamental diffraction limit. However, further theoretical analysis shows that any deviation of the NIM from the ideal cases (lossless) would strongly suppress the superresolution of the subwavelength focal spot. Since both photonic crystals and metals have intrinsic absorptions, the “superlenses” are thus limited to the near field applications.

Another intriguing approach to focus electromagnetic waves is the coherent superposition of unfocused wave fronts. The feasibility of this approach for subwavelength focusing has been experimentally verified

---

\* Corresponding author. Tel.: +0-000-000-0000 ; fax: +0-000-000-0000 .  
E-mail address: [jianfu@zju.edu.cn](mailto:jianfu@zju.edu.cn).

by using a designed apparatus converting 15 laser beams to constitute a converging circular cone [4]. However, the designed apparatus is too complex to be employed into practical applications.

Inspired by this work, my research group proposed a mechanism for subwavelength focusing at optical frequencies based on a tapered microtube fabricated from a glass capillary tube in 2010 [5]. The tapered microtube was fabricated by flame-heated drawing method. When a light beam propagates through the sidewall of the microtube, it converts the input light beam into a circular cone, which forms a subwavelength focusing spot near the output endface. The experimental results reveal the smallest focal spot with a near diffraction-limited full width at half-maximum of  $\sim 435\text{nm}$  ( $0.65\lambda$ ) at a distance of  $\sim 1.47\mu\text{m}$  ( $2.2\lambda$ ) from the output endface of microtube.

In this paper, a further study on subwavelength focusing of light by a tapered microtube is investigated. We analyse the effects of the microtube's taper ratios on focusing in detail. The numerical stimulation demonstrates that the taper of micro-tube has a very direct affect on its focusing effect and when the taper is larger, the focusing spot of the tapered microtube is with higher intensity and smaller full width at half-maximum (FWHM).

## 2. The mechanism of the subwavelength focusing from a tapered microtube

The mechanism to achieve the subwavelength focusing using a tapered microtube is based on the direct synthesis of the angular spectrum of plane waves. According to Fourier Optics, any monochromatic propagating wave can be decomposed to a series of monochromatic plane waves with different wave vectors, which is the theory of angular spectrum decomposition. This theory is well understood and widely used for analysis. It is not as widely recognized, however, that the angular spectrum concept can also be used for synthesis: a focused beam can be synthesized directly from coherent plane waves arranged as a ring in angular spectrum. An ideal Bessel beam with subwavelength diameter can be formed by plane waves as an annular continuous function in the angular spectrum, which makes more energy of outgoing field concentrated in high-frequency components by the frequency band design.

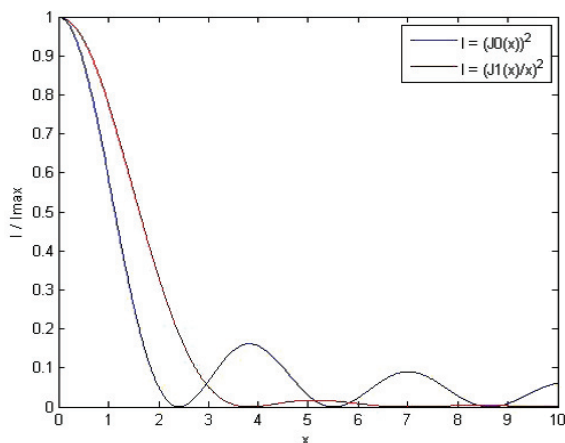


Fig. 1 Intensity distribution of Traditional diffraction limit and the theoretical diffraction limit of the experimental

In the Fig.1, the red line is the intensity distribution of the traditional diffraction limit, which is Airy spot. Airy spot is light intensity distribution synthesized from the angular spectrum of a circular area with a uniform distribution. The blue line is the intensity distribution synthesized from the angular spectrum of annular continuous function. They correspond to the first-order and zero-order Bessel function,

respectively. It can be seen from the figure, the positions of the FWHM of the spot and the first dark ring are compressed. This means that the operation of the angular spectrum can achieve the compression of the diffraction limit and a higher possibility of subwavelength focusing.

An approximate approach is using a finite number of coherent plane waves which have angular spectra distributed uniformly along a ring, yet with rather complicate setup [MIT]. Different from the above method, we use a tapered microtube to achieve Bessel beam with subwavelength focusing. As showed in Fig. 2, this tapered microtube can be easily fabricated from a glass capillary by flame-heated drawing method. The light wave propagating through sidewall of the tapered microtube forms convergent cone with continuous circular angular spectrum distribution. In this way, subwavelength focusing spot can be produced near the output endface. The thickness of sidewall is in the order of the wavelength of light and tapered part is cone-shaped with a ring-shape cross section in the output endface.

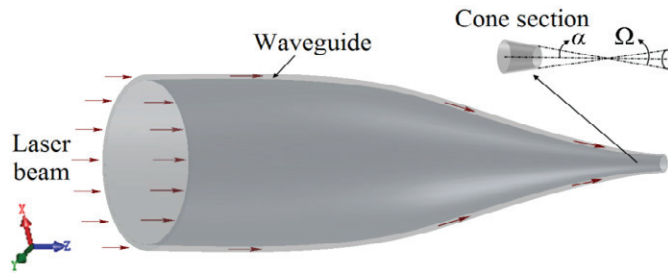


Fig. 2 Schematic of a tapered microtube with a cone section and propagation of waves through the sidewall waveguide of the microtube.  $\alpha$  and  $\Omega$  denote, respectively, half angle and solid angle corresponding to the taper ratio of the cone section.

### 3. Simulation models and Calculation method

In numerical simulation, we have simplified the problem according to the characteristics of this structure and designed effective calculation method for light field of such structures. The structure of the microtube shown in Figure.2 was simplified as a computational model shown in Figure 3. The model consists of three parts, namely, tube region, cone region and the free space. The output light field of each part is the input light field of the next part.

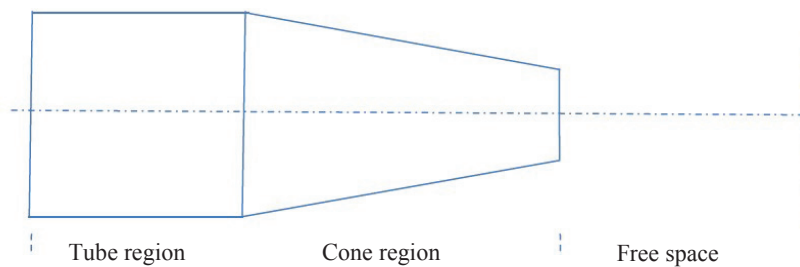


Fig. 3 Simulation model of microtube

In the tube region, we use two-dimensional finite difference time domain (2D-FDTD) to calculate the optical field distribution. Note that, we only calculate the lowest order eigenmodes, because it is most likely to be excited.

In the cone region, we approximated the output optic wave of the endface of the cone region by the coordinate transformation of the output optical field of the tube. As showed in Fig 4, dotted line  $A_1-O_1-B_1$  and  $A_2-O_2-B_2$  is the incident and exit end of the cone region, respectively. We considered the surfaces expressed by the real polyline  $A_1-O'_1-B_1$  and  $A_2-O'_2-B_2$ , which actually were two conical surfaces. Since the two surfaces are perpendicular with the propagation direction of the optical field everywhere, the propagation from  $A_1-O'_1-B_1$  to  $A_2-O'_2-B_2$  is the same with the one in tube region, which can be considered as that the optical field distribution of the surface  $A_2-O'_2-B_2$  is the eigenmode of the optic field of the tube region.

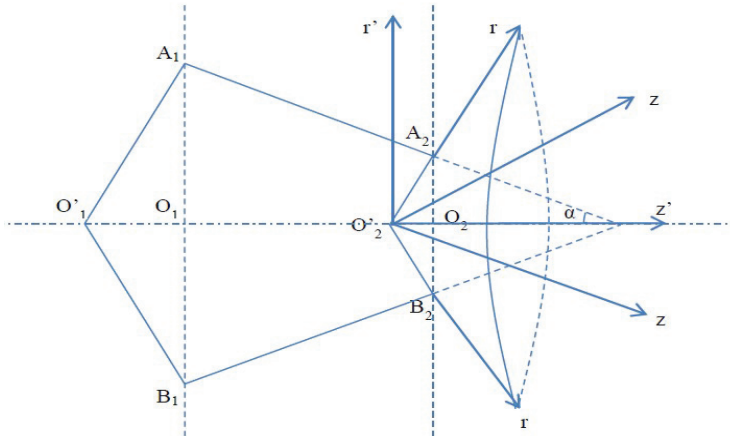


Fig. 4 Calculation and analysis of cone region

When the taper is small, we can assume that  $A_1-O'_1-B_1$  overlaps with  $A_1-O_1-B_1$  and  $A_2-O'_2-B_2$  overlaps with  $A_2-O_2-B_2$ , then the output optic wave of the surface  $A_2-O_2-B_2$  has the same distribution with the one of  $A_2-O'_2-B_2$ , expect that the propagation direction vector  $k$  is not along  $z'$  direction, but still along the  $z$  direction.

We can complete the amendment to the propagation direction by coordinate transformation of the  $k$  space, which is the angular spectrum space, to gain the real output optical wave distribution of the end of cone region. In polar coordinates, intensity space of the light wave and angular spectrum space are related by Fourier transform, which is showed in following.

$$A(k_r, k_\theta) = \int_0^{2\pi} \int_0^\infty E(r, \theta) \exp(i2\pi k_r r \cos(k_\theta - \theta)) r \, dr d\theta, \quad (1)$$

$$E(r, \theta) = \int_0^{2\pi} \int_0^\infty A(k_r, k_\theta) \exp(-i2\pi k_r r \cos(k_\theta - \theta)) k_r \, dk_r dk_\theta, \quad (2)$$

We next consider the problem in angular spectrum space. Shown in the two coordinate systems in Fig.4, assuming the taper of the cone region is  $\alpha$ , we can see that the vectors  $k$  of the angular spectrum distribution of the surface  $A_2-O'_2-B_2$  and  $A_2-O_2-B_2$  satisfy the following relationship.

$$k'_r = k_r \cos \theta - k_z \sin \theta \quad (3)$$

$$k'_z = k_z \cos \theta + k_r \sin \theta \quad (4)$$

Where  $k_z = \sqrt{k^2 - k_r^2 - k_\theta^2}$ ,  $k'_z = \sqrt{k^2 - k_r'^2 - k_\theta^2}$ ,  $k = 2\pi/\lambda$ .

Therefore, as long as getting the angular spectrum distribution of surface  $A_2-O'_2-B_2$ , we can achieve the angular spectrum distribution of surface  $A_2-O_2-B_2$  by coordinate transformation. According to Fourier

optics, the angular spectrum distribution and intensity distribution is corresponding by one to one. Thus, by the method of coordinate transformation in the angular spectrum space, we can use the eigenmode of the light wave in the tube region to get the output optical field distribution of the cone region.

At last in free space, we consider the situation that a given optical field distribution, such as the one in the output end of the cone region, evolves in free space. Similarly, here we consider the use of Fourier optics ideas to analyze the problem.

Accordingly, we still consider the problem in polar coordinates. Assuming the complex amplitude distribution of a given light field as  $E_0(r, \theta)$ , we consider the complex amplitude distribution  $E_z(r, \theta)$  in the distance  $z$  from the output end. In the simplest case of plane waves, assuming  $E_0(r, \theta) = \text{const}$ , we can easily get

$$E_z(r, \theta) = E_0(r, \theta) \cdot \exp(ik_z z), \quad (5)$$

The actual optical field distribution in the beginning of free space can't be plane wave form, but we can make the Fourier transformation to the complex optical field distribution, which is called the plane wave decomposition. Then each plane wave component still satisfies the propagation form of plane wave represented by above equation.

Therefore, assuming that  $A_0(k_r, k_\theta)$  and  $A_z(k_r, k_\theta)$  were the angular spectrum distribution of the endface 0 and endface  $z$ , which can be written as

$$A_0(k_r, k_\theta) = \int_0^{2\pi} \int_0^\infty E_0(r, \theta) \exp(i2\pi k_r r \cos(k_\theta - \theta)) r \, dr d\theta, \quad (6)$$

$$A_z(k_r, k_\theta) = \int_0^{2\pi} \int_0^\infty E_z(r, \theta) \exp(i2\pi k_r r \cos(k_\theta - \theta)) r \, dr d\theta, \quad (7)$$

We can conclude that both satisfy the following relationship according to the physical sense:

$$A_z(k_r, k_\theta) = A_0(k_r, k_\theta) \cdot \exp(ik_z z), \quad k_z = \sqrt{k^2 - k_r^2 - k_\theta^2}, \quad (8)$$

Thus, for any optical field distribution, we can make use of its propagation relationship in angular spectrum space to find the angular spectrum distribution of any surface  $z$ . Using of Fourier inverse transform, we can calculate the complex amplitude distribution at any surface  $z$ .

$$E_z(r, \theta) = \int_0^{2\pi} \int_0^\infty A_z(k_r, k_\theta) \exp(-i2\pi k_r r \cos(k_\theta - \theta)) k_r dk_\theta, \quad (9)$$

#### 4. Result of the numerical calculation

We utilize above numerical method to investigate the effect of the taper ratio of microtube. We take the diameters of the output as  $2.5\mu\text{m}$ , thickness of the tube as  $0.15\mu\text{m}$ , the refractive index  $n$  as 1.45, and wavelength as  $671\text{nm}$ . The half angle of the taper is taken as  $0^\circ$ ,  $5^\circ$ ,  $10^\circ$  and  $15^\circ$ , respectively, to study the propagation properties in the free space and the focusing effect as showed in Fig. 5.

It can be clearly seen in Fig. 5 that the existence of the taper results in the smaller focusing spot and better focusing effect. Fig.6 shows the angular spectrum distribution of the output light wave from the two tapered microtube whose taper ratios is  $0^\circ$  and  $5^\circ$ , respectively. It can be seen in the angular spectrum distribution that the taper makes energy move to the high frequency components, which means a further compression of the traditional diffraction limit.

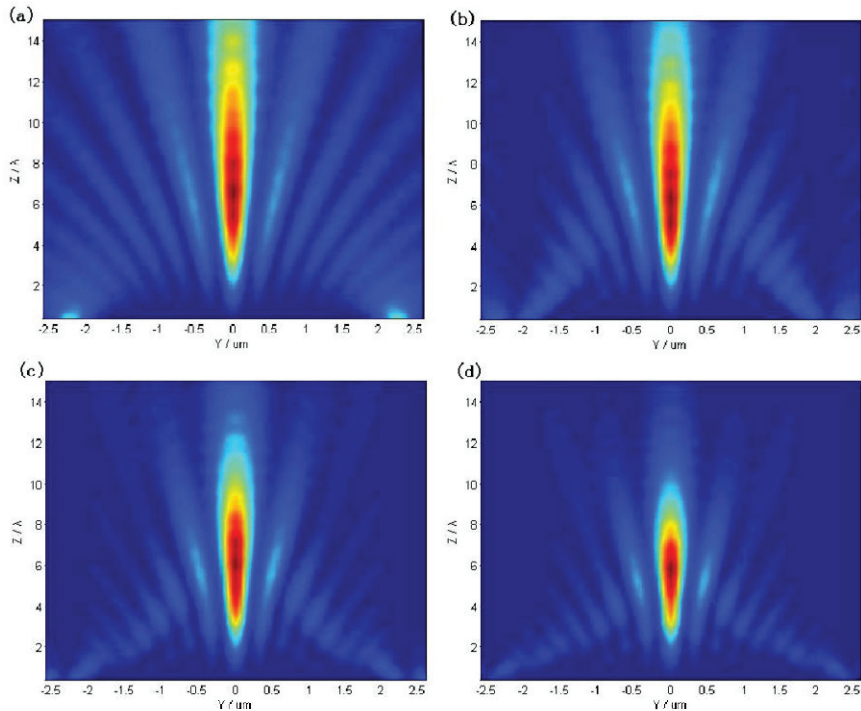


Fig.5. Optical field distribution of different taper of microtubes; (a)  $0^\circ$ ; (b)  $5^\circ$ ; (c)  $10^\circ$ ; (d)  $15^\circ$

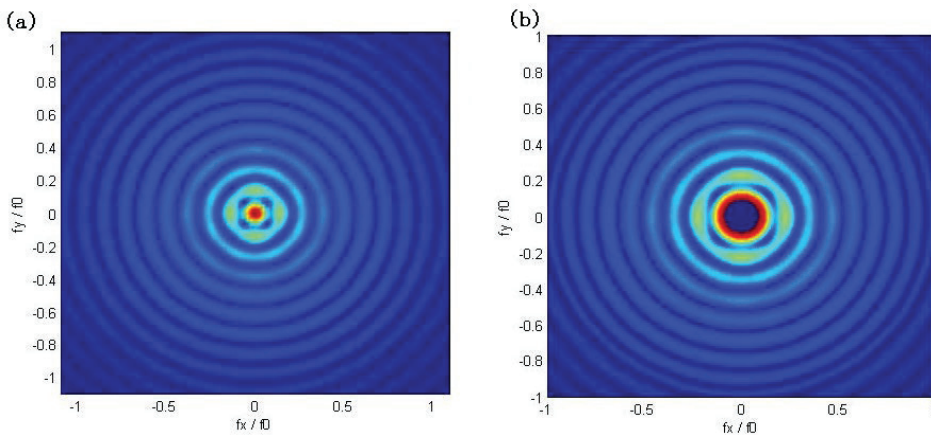


Fig. 6 Angular spectral distribution of light different taper angle of microtube; (a)  $0^\circ$ ; (b)  $5^\circ$

From Fig. 5, we can also find that as the taper ratios increases, the energy of focusing light gradually concentrates to the central axis and the length of the spindle-like focusing region, which means the larger the taper angle, and the greater capacity of microtube to focus and the smaller the FWHM value of focused spot formed.

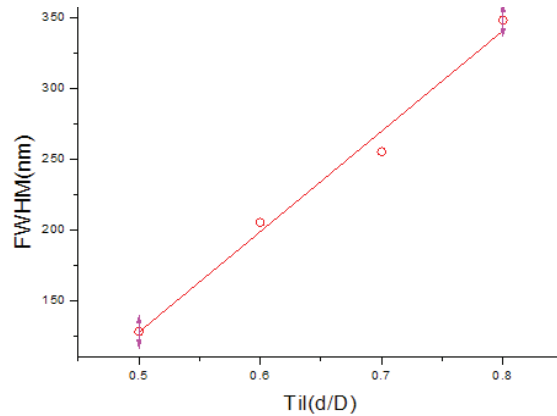


Fig. 7. The FWHM of focal spot as a function of Til

To see more clearly the influence of the taper ratios on the focusing effect, we take the length of the taper as  $1\mu\text{m}$  and use the Til ( $\text{Til}=d/D$ ) to characterize the taper ratios where  $d$  and  $D$  are the diameters of the output and input ends, respectively. The smaller the Til is, the greater the taper ratios. We take  $d$  as  $2.5\mu\text{m}$ , thickness of the tube as  $0.15\mu\text{m}$ , the refractive index  $n$  as 1.45, and wavelength as  $671\text{nm}$ . The FWHM of the focal spot is calculated, and plot as a function of Til in Fig. 7. It shows approximately a linear relation, with subwavelength spot sizes within the plot range.

As we can see from the results presented above, the taper of micro-tube has a very large impact on the focal spot size. Though bigger taper is better, it is difficult to prepare such sample with low propagation loss. In addition, the changes of the taper hardly have any impact on focus distance, which is always maintained at about  $2\mu\text{m}$ .

## 5. Conclusions

To achieve the subwavelength focusing by a microtube is a new mechanism. This focusing effect is influenced by many factors. From numerical simulation, it can be seen that the role of taper ratios is very important and when the taper is larger, the focusing spot has smaller FWHM.

## Acknowledgements

This work is supported by the National High Technology Research and Development Program (“863” Program) of China (2011AA120101).

## References

- [1] D. G. Grier, *Nature Photonics* **424**, 21 (2003).
- [2] B. D. Terris, H. J. Mamin, and D. Rugar, *Appl. Phys. Lett.* **68**, 141 (1996).
- [3] J. B. Pendry, *Phys. Rev. Lett.* **85**, 3966 (2000).
- [4] S. S. Hong, B. K. P. Horn, D. M. Freeman, and M. S. Mermelstein, *Appl. Phys. Lett.* **88**, 261107 (2006).
- [5] Jian Fu, Hongtao Dong, and Wei Fang, *Appl. Phys. Lett.* **97**, 041114 (2010)